

Development of Micro-Permanent Magnet Synchronous Reluctance Generator for TPMS on Smart Robots

Chun-Chieh Chang, Cheng-Tang Pan, Shao-Yu Wang, An-Yun Yang, Gu-Xuan Lin, Yu-Jen Wang
National Sun Yat-sen University, Kaohsiung, 80424, Taiwan
panct@mail.nsysu.edu.tw

Roger Chenglung Lee, Ting-Hung Chung
Naroller Electronics, Kaohsiung, 80424, Taiwan
335i2007@gmail.com

Abstract

Synchronous Reluctance Generator (SynRG) is a stability and robust motor with simple structure and low cost. In this paper, the SynRG which embedded magnet was used in tire pressure monitoring system (TPMS). The slot-pole ratio was analyzed to obtain greater generating capacity, minimize cogging torque and torque ripple. A wide selection of surface permanent magnet generator (SPMG) was compare with PM-SynRG. The results show that the generating capacity of PM-SynRG was more than 3 V with high degree of stability in the operation.

Keywords: Magnet synchronous reluctance generator, Tire pressure monitoring system

1. Introduction

Synchronous reluctance generators (SynRG) have been widely used in industries such as energy, integration - starter generator (ISG), and wind turbines [1-3]. In general, an optimization characteristics of SynRG are defined as the maximum induced voltage, the minimum cogging torque, the maximum efficiency, and the maximum power factor. There are many studies on SynRG in a wind turbine power generating system [4-7]. SynRG has a robust and low price due to its simple rotor structures. In addition, SynRG is applies to variable speed operation, because of its low noise. In the most popular hybrid electric vehicle (HEV), there are many studies of SynRG to replace permanent magnet generator (PMG) [8,9]. The permanent magnet synchronous reluctance generator (PM-SynRG) was applied to micro-generator due to low cost, high efficiency and stability. Especially in the smaller size of the generator, a large torque ripple easily leads to the obstruction of rotation.

In this paper, the PM-SynRG which embedded magnet was used in tire pressure monitoring system (TPMS). It has a stable generating capacity and robust

structure. In the experiment, a wide selection of surface permanent magnet generator (SPMG) was compare with PM-SynRG to confirm the performance. Figure 1 shows the schematic of the winding structure and the rotor structures. There are plenty of magnet materials where the selection of magnet material needs to be considered carefully. The NdFeBr was selected because of the magnet undesired demagnetization [10]. The ratio of the slot and pole and the winding distribution were also analyzed in this paper. In addition to a larger amount of power, the cogging torque and torque ripple was concerned.

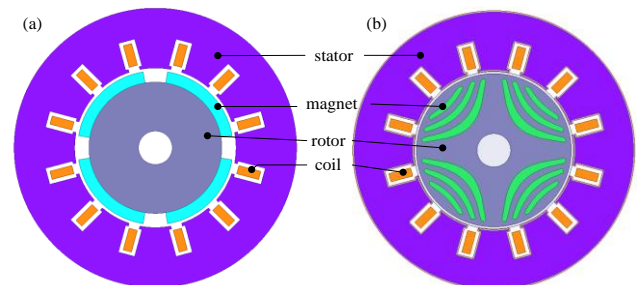


Figure 1 Schematic diagram of (a) SPMG and (b) PM-SynRG

2. Experimental Methods

2.1 Design specifications

Finite element method (FEM) was used for the magnetic circuit analysis, including the B-EMF, B-EMF waveform, torque, and torque ripple. In the structural design, as shown in table 1, the number of coils was considered to the size of generator, and the 400 turns was calculated. An air gap between the rotor and the stator was set at 0.55 mm, and rotational speed is 500 rpm.

The critical properties of permanent magnets for permanent magnet generators are high BH energy. The commercial magnet, Nd₂Fe₁₄B, have coercive force approaching 890 (kA/m). To operate the PMG with permanently excited PM poles at variable power factors is concerned.

Table 1 Specification List

Item(Unit)	Value	
	SPMG	SynRG
Type of machines		
Stator poles numbers	12, 24	
Rotor poles numbers	4, 8, 10	
Stator outer radius(mm)	50	
Stator inner radius(mm)	28.6	
Airgap length(mm)	0.55	
Axial length(mm)	5	
Turns per coil	400	
Magnet remanence(T)	1.23	
Coercive force of PM(kA/m)	890	
Rated speed(rpm)	500	
Load Resistance(ohm)	100	

2.2 Permanent magnet synchronous machine

The equations for the permanent magnet synchronous machine in the d-q-components were shown below [11],

$$\mu_{sd} = R_S i_{sq} - \omega_{el} L_d i_{sd} \quad (1)$$

$$\mu_{sq} = R_S i_{sq} + \omega_{el} L_d i_{sd} + \omega_{el} \phi_m \quad (2)$$

where μ_{sd} and μ_{sq} are the stator voltage in d and q axis, R_S is the armature phase resistance, ω_{el} is the electrical speed, L_d is the d-axis inductance, L_q is the q-axis inductance, i_{sd} and i_{sq} are the stator current in d and q

axis respectively and ϕ_m is the flux linkage originating from the magnets.

The torque is formed as

$$T = \frac{3}{2} P [\phi_m i_{sq} + (L_d - L_q) i_{sq} i_{sd}] \quad (3)$$

where p is the number of pole pairs.

2.3 Winding design

There are a lot of feasible combinations of stator and rotor pole numbers in multiphase PM machines, viz.,

$$N_s = k_{1m}, k_1 = 1, 2, \dots \quad (4)$$

$$N_r = N_s \pm k_2, k_2 = 1, 2, \dots \quad (5)$$

where N_s and N_r are the number of stator and rotor poles, respectively, and m is the number of phases. k_1 is an integer number when m is an even number, but k_1 should be an even number when m is an odd number, since the number of stator poles must be even, which is different from the conventional fractional-slot PM machines [12].

2.3.1 Calculation of the span θ_s of per slot is

$$\theta = \frac{N_p \times 180^\circ}{N_s} \quad (6)$$

2.3.2 Calculation of the phase offset 120° E that the required number of slots (K_o) is

$$K_o = \frac{120^\circ + q \times 360^\circ}{\theta_s} \quad (7)$$

Where $q = 1, 2, \dots, (Np/2 - 1)$, Phase offset of slot pitch K_o . When unable to find a suitable integer K_o , that means that the selected number of poles and stator slots feasible combination, and to be re-selected.

The 120° means that each of phase is a gap of 120° degrees; $q * 360 / \theta_s$ means to find in all phases of a coil, and it could sense the same voltage waveform in a cross slot pitch

2.3.3 Select the number of slots spans of coil S^*

$$S^* = \max[\text{fix}(\frac{180}{\theta_s})] \quad (8)$$

The fix (.) is the maximum of two numbers in the integer part. All the slots are numbered along the direction of rotation of the generator.

2.4 Calculation of the torque ripple

Back electromotive force (B-EMF) waveform was analyzed above. When the generator was rotated, the torque was produced. The torque ripple was calculated in each of slot, poles of combination as defined in (9):

$$T_{rip}(\%) = \frac{T_{max} - T_{min}}{T_{avg}} \times 100\% \quad (9)$$

where T_{max} is the maximum torque, T_{min} is the torque minimum, and T_{avg} is average torque.

3. Simulation Analysis

FEM was used for the magnetic circuit analysis, including the B-EMF, B-EMF waveform, torque, and torque ripple.

3.1 Analysis of Back Electromotive Force(B-EMF)

Figure 2 shows that the generating capacity of SPMG is greater than PM-SynRG, because the flux of the SPMG was no obstacle in rotor. In the study, when the number of poles was increased gradually, the generating capacity of PM-SynRG was decreased; when the number of poles gradually was increased, the generating capacity of SPMG was increased. On the other hand, the number of slots was increased, generating capacity of PM-SynRG are also increased. The result above in the poles 10 poles, the 12 and 24 slots generating capacity were almost the same. When the number of slots of SPMG is increased to 24 slots, power generating capacity is not significantly increased. Figure 3 shows a B-EMF waveform diagram, B-EMF waveform was observed to exhibit a concave or flat shape of the peak, when the number of slots with pole number is less. The reason was that when the number of slots and poles was small, each slot of each phase coil which induced B-EMF was different. When all are combined, B-EMF will form a non-sinusoidal shape. Generator was stabilized and enhanced the efficiency of the operation due to the output is close to the sine wave. Although the generating capacity of PM-SynRG is

smaller than SPMG, the generating capacity of micro generators was reached that more than 3 V.

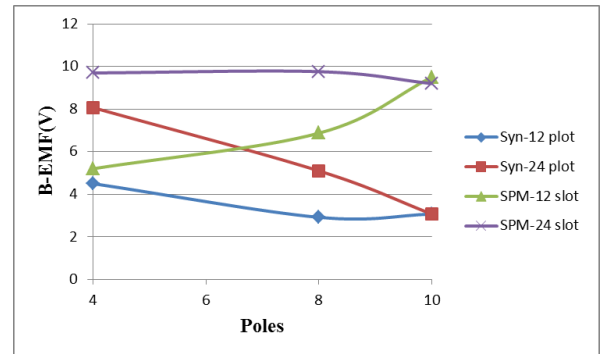


Figure 2 B-EMF of comparison of two types of generators

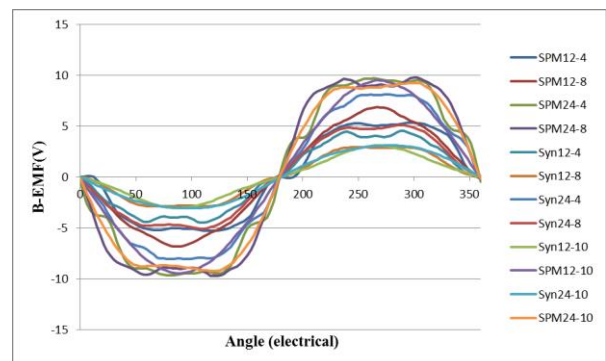


Figure 3 B-EMF waveform of comparison of two types of generators

3.2 Torque Analysis

Figure 4 shows that SPMG torque magnitudes were larger than the PM-SynRG and the gap was even greater with the increase of the number of poles. The reason was the structure of PM-SynRG had a high degree of stability during operation. The torque magnitudes of PM-SynRG were gradually reduced with the increase of the number of poles; the torque magnitudes of SPMG were gradually increased with the increase of the number of poles. Figure 5 shows a waveform diagram of torque and it was found that SPMG torque ripple was greater than the PM-SynRG. Both torque ripples were smaller with the increase of the number of slots and poles. From the above analysis, torque and torque ripple of PM-SynRG were less than SPMG. In particular, the generating capacity was less than 4V and the trend increasingly obvious.

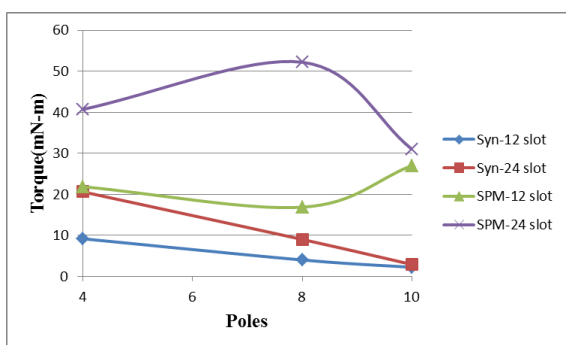


Figure 4 Torque of comparison of two types of generators

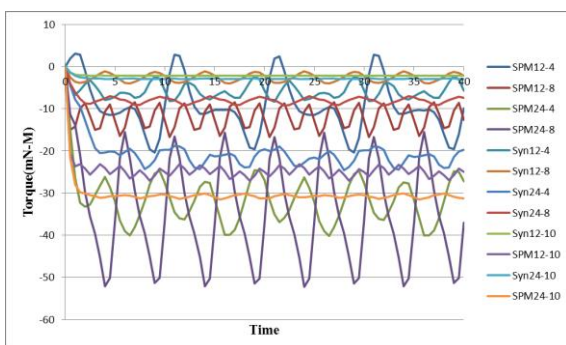


Figure 5 Torque ripple of comparison of two types of generators

4. Conclusions

In the paper, the PM-SynRG was applied to the TPMS to achieve a stable and robust power generating structure. The ratios of slot-pole number were analyzed to obtain greater power generating capacity and decrease cogging torque and torque ripple. The results show that generating capacity of PM-SynRG was more than 3 V. In the torque magnitude and torque ripple, PM-SynRG was less about 3 times than SPMG with high stability. For micro tire pressure detectors required performance, PM-SynRG was achieved the requirement for generating capacity and has a high degree of stability in the operation.

References

1. S. Tokunaga, K. Kesamaru. "FEM simulation of novel small wind turbine generating system with synchronous reluctance generator", *Electrical Machines and Systems (ICEMS)*, 2011.
2. M.A. Rahman, "Advances of Interior Permanent Magnet (IPM) Wind Generators", *Electrical Machines and Systems*, 2008, pp. 2228 - 2233.

3. Erko Lepa and Aleksander Kilk, *Analysis and Prototyping of a Low-Speed Small Scale Permanent Magnet Generator for Wind Power Applications*, *Electric Power Quality and Supply Reliability Conference (PQ)*, 2012.
4. S. Morimoto, H. Kato, M. Sanada and Y. Takeda, "Output Maximization Control for Wind Generating System with Interior Permanent Magnet Synchronous Generator", *Proceedings of IEEE – IAS Annual Meeting, Tampa, FL, October 4-8, 2006*, pp. 503-510.
5. S. Morimoto, H. Nakayama, M. Sanada and Y. Takeda, "Sensorless Output Maximization Control for Variable-Speed Wind Generating System using IPMSG", *IEEE Transactions on Industry Applications*, Vol. 41, No. 1, 2005, pp. 60-67.
6. Dept. of Electr. & Comput. Eng., Texas A&M Univ., College Station, TX, "Maximum output power control of permanent magnet-assisted synchronous reluctance generator", *ICEM*, 2008.
7. Urase, K., Tokyo, Kiyota, K., Sugimoto, H., Chiba, Design of a Switched Reluctance Generator Competitive with the IPM Generator in Hybrid Electrical Vehicles, *Electrical Machines and Systems (ICEMS)*, 2012.
8. Poopak Roshanfekar, Sonja Lundmark, Torbjörn Thiringer, and Mikael Alatalo, "A Synchronous Reluctance Generator for a Wind Application- Compared with an Interior Mounted Permanent Magnet Synchronous Generator", *Power Electronics, Machines and Drives (PEMD)*, 2014.
9. Dept. of Electr. & Comput. Eng., Texas A&M Univ., College Station, TX, "Optimal design and comparison of stator winding configurations in permanent magnet assisted synchronous reluctance generator", *Conference: Electric Machines and Drives Conference*, 2009.
10. M. Katter, "Angular Dependence of Demagnetization Stability of Sintered Nd-Fe-B Magnets," *IEEE Transactions on Magnetics*, Vol. 41, 2005, pp. 3853-3855.
11. J. T. Chen, and Z. Q. Zhu, "Winding configurations and optimal stator and rotor pole combination of flux-switching PM brushless AC machines," *IEEE Trans. Energy Conversion*, vol. 25, no. 2, 2010, pp. 293-302.
12. D. Ishak, Z. Q. Zhu, and D. Howe, "Comparison of PM brushless motors, with either all or alternative wound teeth," *IEEE Trans. Energy Convers.*, vol. 21, no. 1, 2006, pp. 95-103.